

Oxidation of styrene to benzaldehyde and styrene oxide over nickel and copper ceria solution combustion catalysts

*Qinisani Gazu*¹, *Mzamo Shozi*¹, and *Philani Mpungose*^{2*}

¹School of Chemistry and Physics, University of KwaZulu-Natal, Durban, 4000, South Africa

²Department of Chemistry, Cape Peninsula University of Technology, Cape Town, 2000, South Africa

Abstract. CeO_2 , $\text{Cu}_{0.05}\text{Ce}_{0.95}\text{O}_{2-\delta}$, $\text{Ni}_{0.04}\text{Ce}_{0.96}\text{O}_{2-\delta}$, $\text{Cu}_{0.05}\text{Ni}_{0.05}\text{Ce}_{0.90}\text{O}_{2-\delta}$, catalysts were synthesised via solution combustion technique using urea as a fuel. The as pre-prepared catalysts were characterised via X-ray powder diffraction, Brunauer-Emmett-Teller surface area analysis, transmission and scanning electron microscopy analysis. The characterisation techniques strongly suggested that all the catalysts were prepared successfully, and that copper and nickel were successfully incorporated into the lattice structure of ceria. The effect of the reaction conditions on the catalytic properties of the synthesised material were studied in detail using $\text{Cu}_{0.05}\text{Ni}_{0.05}\text{Ce}_{0.90}\text{O}_{2-\delta}$ as the model catalyst. The effect of temperature, solvents and co-oxidants was investigated in optimisation studies. A combination of acetonitrile, tert-butyl hydroperoxide and a temperature of 60 °C were found to be optimal after 24 hours and used for all catalysts. All catalysts were found to be active in styrene oxidation under these conditions, with styrene conversion as high as 69% over $\text{Ni}_{0.04}\text{Ce}_{0.96}\text{O}_{2-\delta}$, and selectivity to benzaldehyde and styrene oxide 38 and 26% respectively.

1 Introduction

In the synthesis of advanced nanomaterials and catalysts, combustion synthesis (CS) has been determined as an important technique [1-8]. This synthesis utilises the exothermicity of reduction-oxidation reactions to produce useful materials. The advantage of the CS method over other synthesis methods are: (i) use of simple equipment, (ii) it produces high-purity products, (iii) the stabilisation of metastable phases and, (iv) produces any size and shape of products [8]. A variety of metal oxides are prepared using solution combustion (SC). Metal oxides with interesting magnetic, dielectric, electrical, mechanical, catalytic, luminescent and optical properties have been synthesised [9]. By SC the composition, structure of prepared oxide materials can be easily controlled [8,9]. Fuels play an important role in SC because they drive the exothermicity of the reaction. The nature of combustion can vary from flaming to non-flaming depending on the fuel used and the exothermicity of the redox reaction can vary between 1000 to 1800 K [10-16].

* Corresponding author: mpungosep@cput.ac.za

The attraction to catalytic oxidation of styrene over heterogeneous catalysts to produce valuable chemicals has been influenced by the need to develop methods that produce less or no hazardous reaction wastes [17-21]. Of huge importance in the oxidation of styrene, is the production of benzaldehyde which is used in the perfume industries, the production pharmaceuticals, dye stuffs, and agrochemicals [22-24]. Styrene oxide also produced in styrene oxidation is used in the production of epoxy resin diluting agents, ultraviolet adsorbents, flavouring agents, etc. and also, it is an important intermediate in organic synthesis, pharmacology and perfumery [17].

The use of heterogeneous mixed metal catalysts in the oxidation of styrene using tert-butyl hydroperoxide (TBHP) and H_2O_2 as co-oxidants has been reported [17, 22, 24-25]. Main products observed were benzaldehyde and styrene oxide. Of interest to our study was work previously reported by Valand *et al.* [19]. They studied styrene oxidation at 40 °C using TBHP and H_2O_2 as co-oxidants over mixed Cu–Ni–Co nano-metal oxides catalysts prepared via ultrasonic cavitation-impregnation. TBHP showed a better conversion (73%) than H_2O_2 (42%) which was obtained when styrene:oxidant molar ratio was 1:1.5 with selectivity to benzaldehyde and styrene oxide being 73 and 20% respectively. There is little literature on styrene oxidation over ternary metal oxide catalysts. This study evaluates the oxidation of styrene using copper, nickel and ceria ternary catalysts prepared by solution combustion, which has not been previously reported.

2 Experimental

Catalyst preparation. CeO_2 , $Cu_{0.05}Ce_{0.95}O_{2-\delta}$, $Ni_{0.04}Ce_{0.96}O_{2-\delta}$ and $Cu_{0.05}Ni_{0.05}Ce_{0.90}O_{2-\delta}$ catalysts were prepared using a single-step solution combustion method. A redox combustion mixture was prepared by mixing (6.86 mmol) urea (Sigma-Aldrich, 99.9%) and (19.0 mmol) $(NH_4)_2Ce(NO_3)_6$ (Sigma-Aldrich, 99.9%) in a fuel:oxidant ratio of 4:1. This was done in a borosilicate dish in 40 mL of distilled water. The mixture was heated while stirring to evaporate water and form a slurry. The mixture was then transferred to a muffle furnace preheated to 120 °C and the temperature was increased to 400 °C. The mixture was left to combust for 5 hours then the catalyst was removed as the product. For the Cu and Ni catalysts, $Cu(NO_3)_2 \cdot 3H_2O$ (Sigma-Aldrich, $\geq 97\%$) and $Ni(NO_3)_2 \cdot 6H_2O$ (Sigma-Aldrich, $\geq 97\%$) were used as oxidants respectively in combination with $(NH_4)_2Ce(NO_3)_6$ in the molar ratio stipulated in their chemical formula, with the fuel:oxidant ratio always kept at approximately 4:1. From hereon, the synthesised catalysts CeO_2 , $Cu_{0.05}Ce_{0.95}O_{2-\delta}$, $Ni_{0.04}Ce_{0.96}O_{2-\delta}$ and $Cu_{0.05}Ni_{0.05}Ce_{0.90}O_{2-\delta}$ will be referred to as CeO, CuCeO, NiCeO and CuNiCeO respectively.

Catalyst characterization. BET surface area, pore volume and pore size were measured from the adsorption and desorption isotherms of nitrogen using a Micromeritics TriStar II Surface area and Porosity Analyzer. About 0.3 g of each powder sample was degassed overnight at 200 °C using a Micromeritics FlowPep 060 instrument prior to analysis.

Metal composition was determined by analysis on a PerkinElmer Optical Emission Spectrometer Optima 5300 DV. The standards (1000 ppm Ce and Pd) were purchased from Fluka.

Powder X-ray diffraction (XRD) studies were conducted on a Bruker D8 Advance diffractometer with Cu ($K\alpha$, $\lambda = 1.5406 \text{ \AA}$) as the radiation source.

Transmission electron microscopy (TEM) was performed on a Jeol JEM-1010 electron microscope. The powder samples were ultrasonically dispersed in ethanol and supported on a perforated carbon film mounted on a copper grid prior to analysis.

A ZEISS FEG-SEM UltraPlus instrument was used to obtain scanning electron microscopy (SEM) images. The analysis was performed at random points along the surface of the catalyst. The samples were first mounted on aluminium stubs using double-sided carbon tape; they were then coated with gold using a Polaron E5100 coating unit.

Catalytic oxidation of styrene. Reactions were carried out in a Schlenk tube fitted in an oil bath and the reaction temperatures were monitored. An amount of 50 mg of CuNiCeO and 0.5 mmol styrene were used to carry out optimization reactions. Optimization was carried out by varying solvents: acetonitrile, tert-butanol and water; co-oxidants: TBHP, H₂O₂ and NaIO₄ as well as their equivalents and temperature: room temperature, 40 °C and 60 °C. The optimum conditions were used to carry out testing for the oxidation of styrene over synthesized catalysts. Reactions were monitored every 2 hours for 12 hours then after 24 hours. Product identification and quantification was done using a Perkin Elmer Clarus 500 GC equipped with an FID and a PONA column.

3 Results and discussion

Catalyst characterization. Table 1 shows the physical and textural properties of the catalysts. The metal content shows that the catalysts were successfully synthesised with the intended molar ratio. When the copper and nickel were incorporated into the ceria lattice, there was a decrease in the pore volume. The average crystallite size was found to be 10 nm for the catalysts.

The x-ray powder diffractograms of the catalysts are shown in Figure 1. The diffraction peaks of all the catalysts can be indexed to the fluorite structure of CeO₂ [26]. All diffractograms are similar to that of the blank CeO₂ which confirms successful incorporation of nickel and copper atoms into the ceria lattice. The absence of the Cu⁰, Ni⁰, CuO and NiO phases in the XRD patterns of the CuNiCeO, NiCeO, CuCeO samples suggests that the Cu²⁺ and/or Ni²⁺ ions were successfully incorporated into the ceria lattice. The incorporation of the Cu²⁺ and/or Ni²⁺ into the ceria lattice came with the expected physicochemical changes to ceria. The peak for the [111] plane shifts to lower 2 theta values upon the introduction of Cu²⁺ and/or Ni²⁺ into the ceria lattice (Figure 1 insert). This shift is associated with increases in lattice parameters that cause the ceria lattice to be strained [27].

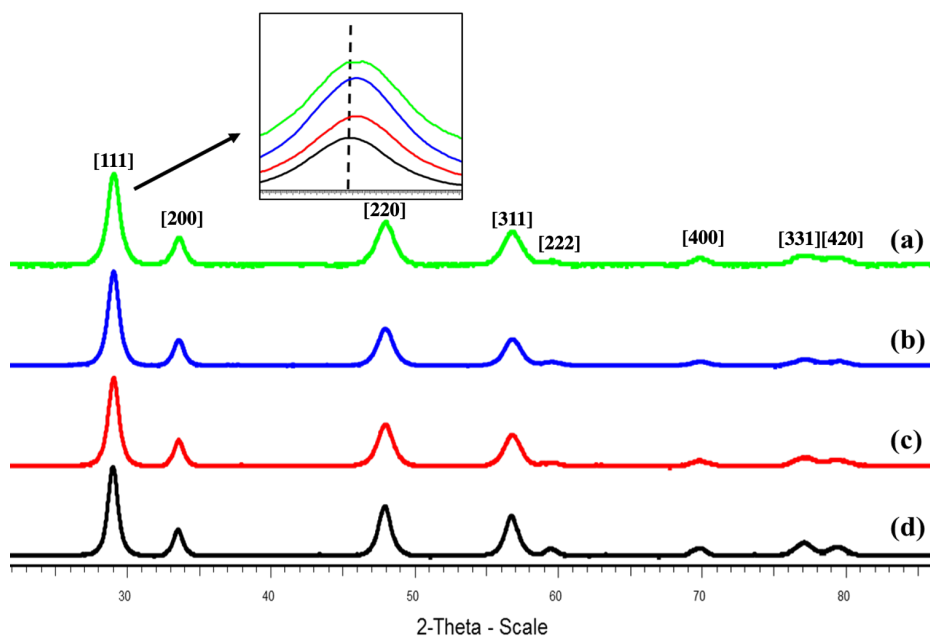


Fig. 1. X-ray powder diffractograms of (a) CuNiCeO, (b) NiCeO, (c) CuCeO and (d) CeO with an insert of magnification of peaks at a 2θ value of 29°.

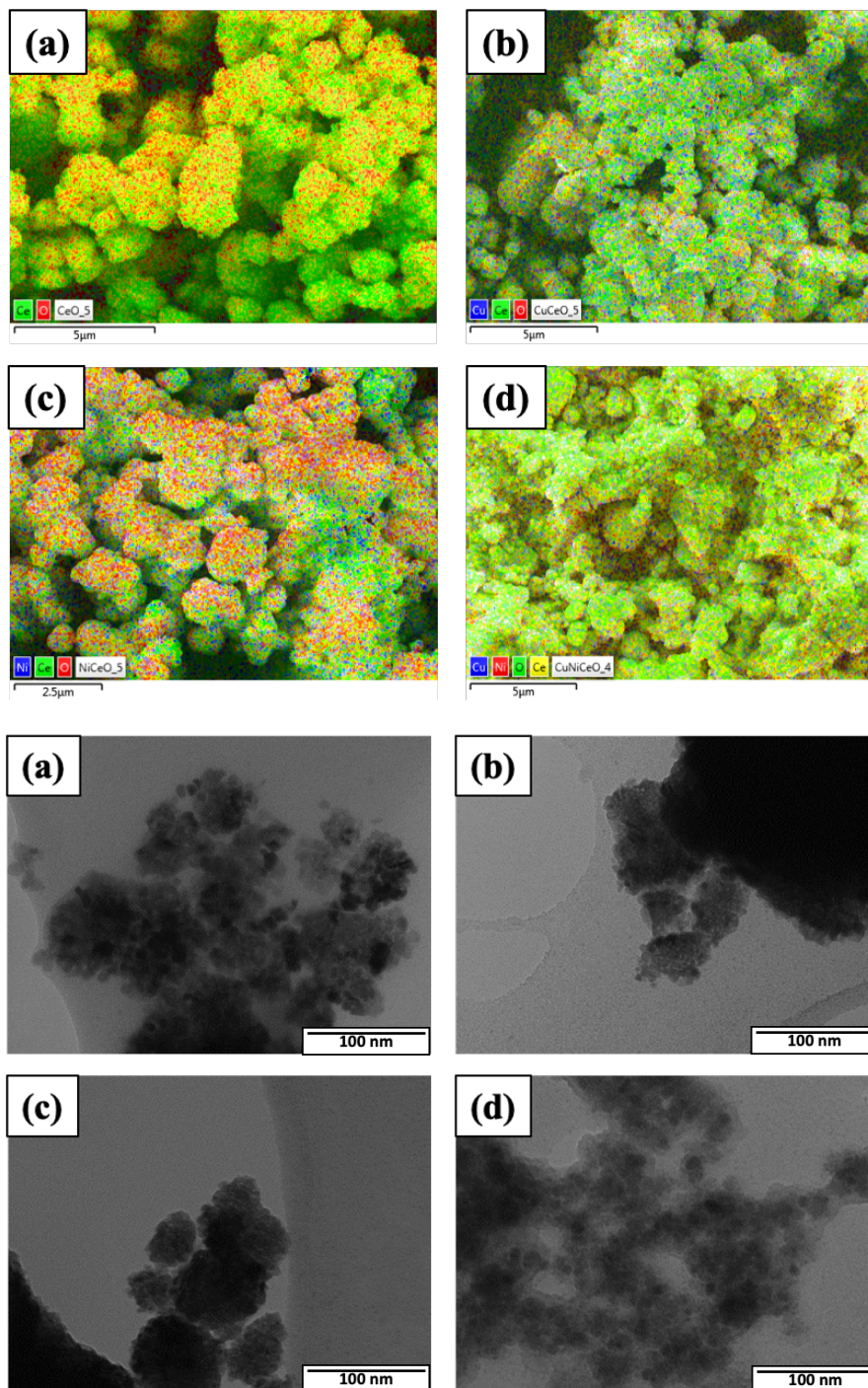


Fig. 2. SEM-EDX (top) and TEM (bottom) images of (a) CeO, (b) CuCeO, (c) NiCeO and (d) CuNiCeO.

Table 1 Physical and textural properties of the catalysts

Catalyst	Metal content (mol%)			S _{BET} * (m ² /g)	Pore volume (cm ³ /g)	Crystallite size [#] (nm)
	Ce	Cu	Ni			
CeO ₂	100	-	-	49	0.042	11
CuCeO	95	5	-	45	0.029	10
NiCeO	96	-	4	54	0.035	9.6
CuNiCeO	90	5	5	25	0.023	9.0

*S_{BET} = BET surface area.

[#]Average crystallite sizes as determined from the FWHM of the peaks using the Scherer equation

Figure 2 shows the SEM-EDX and TEM images of the prepared catalysts. The morphology of all catalysts is similar and consists of spherically-shaped particles. The metal oxide particles are evenly distributed as observed in the SEM images which suggests that synthesis of catalysts via SC yields materials with good dispersion. TEM images also show that the particles are spherical in nature and are approximately 10 nm in size which is in agreement with the average crystallite size determined via XRD (Table 1).

Catalyst testing: Optimization. Figure 3 shows the optimization data for the oxidation of styrene for 24 hours using 50 mg CuNiCeO as the catalyst. For solvent optimization (Figure 3a), TBHP was used as the co-oxidant as this has been reported to be ideal for these type of reactions [19, 28]. The highest conversion (95%) was obtained when acetonitrile was used as a solvent followed by *t*-butanol (52%). The selectivity to benzaldehyde and styrene oxide when acetonitrile was used a solvent was found to be 20 and 21% respectively. No activity was observed using water as a solvent due to poor miscibility with styrene.

Acetonitrile was then chosen as solvent for co-oxidant optimization (Figure 3b). No activity was observed using H₂O₂ and NaIO₄ as H₂O₂ has been reported to decompose at temperatures greater than 30 °C [28-29] while NaIO₄ may have encountered poor solubility as no water was added to the reaction. Generally, NaIO₄ shows good activity when used in a acetonitrile/water solution [30]. TBHP achieved a 95% styrene conversion with selectivity to benzaldehyde and styrene oxide being 20 and 21% respectively.

The TBHP equivalents to styrene were then investigated (Figure 3c) and the highest conversion (96%) was obtained when 10 equivalents were used at the expense of formation of benzaldehyde and styrene oxide which oxidised further to benzoic acid and acetophenone [19, 31]. The optimum equivalents were chosen to be 3 as a high conversion (90%) was also obtained. Temperature was optimized using acetonitrile as the solvent and 3 equivalents of TBHP (Figure 3d). The highest conversion (95%) was obtained at 60 °C with selectivity to benzaldehyde and styrene oxide being 57 and 21% respectively.

Styrene oxidation over prepared catalysts. The results from catalyst testing can be seen in Figure 4. The CeO catalyst gave the lowest conversion (40%) which increased with substitution of Ni or Cu in the ceria lattice. NiCeO giving the highest conversion (69%) and this could be due to NiCeO having the largest surface area amongst the catalysts and therefore an increased availability of metal oxide active sites. The second highest conversion (61%) was observed when no catalyst was present. Having no catalyst meant the reaction system was homogeneous and such systems have been previously reported to yield good activity due to fast reaction rates [32]. Generally, the selectivity to styrene oxide was found to be higher than that to benzaldehyde and similar observations were made by Liu *et al.* over their ceria

catalysts [33]. For all catalysts, there was a higher selectivity to other products (~54 – 72%) such as benzoic acid, 1-phenylethane-1,2-diol, acetophenone and phenyl acetaldehyde which result from the over-oxidation of benzaldehyde and styrene oxide. This could imply that TBHP is a harsh co-oxidant for this system and the catalysts are not very selective to the desired products.

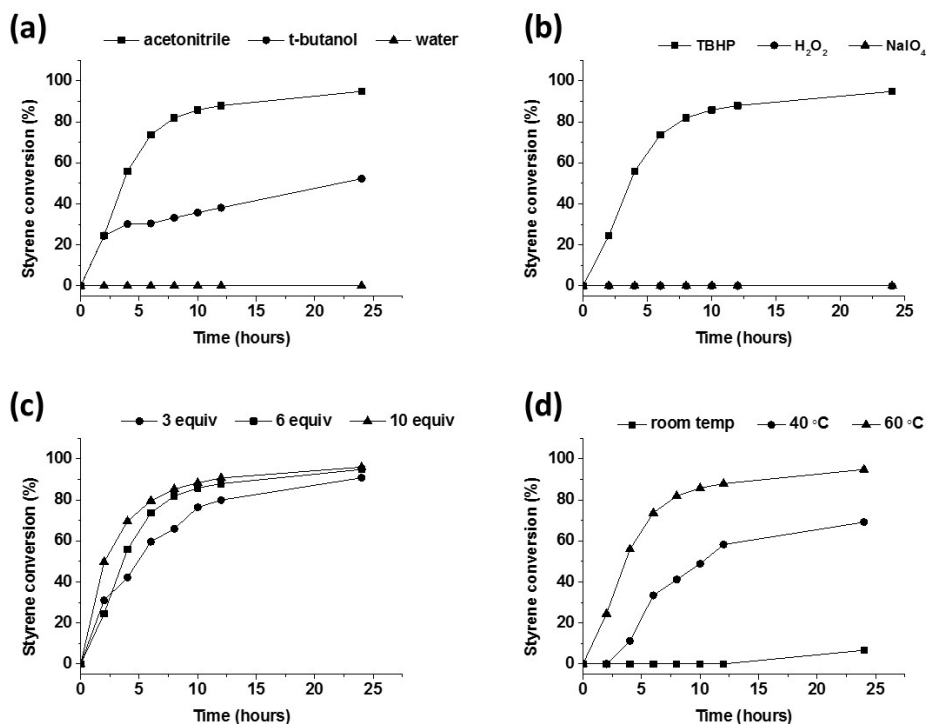


Fig. 3. (a) Solvent optimization at 60 °C using 3 equiv. TBHP, (b) co-oxidant optimization at 60 °C using optimized solvent (acetonitrile), (c) optimization of TBHP equivalents to styrene using acetonitrile at 60 °C and (d) temperature optimization using acetonitrile and 3 equiv. TBHP.

The mechanism of styrene oxidation over heterogeneous catalysts using TBHP as the co-oxidant has been reported to proceed by molecules of styrene and TBHP adsorbing on the catalyst surface, with the catalyst controlling the breaking and formation of bonds to produce products from styrene [19, 31,34]. Campbell and Peden [35] previously reported that the active sites in ceria catalysts lies in Ce³⁺ ions that are coupled with large sized oxygen vacancy clusters. These vacancies activate the substrate thereby improving catalytic performance. Liu *et al.* [36] proposed a mechanism whereby styrene oxidation occurs over the surface of the ceria catalyst with styrene being adsorbed onto the surface. Styrene undergoes oxidation by reaction with the highly reactive oxygen species at the oxygen vacancy site. Products are generated and the remaining oxygen vacancies are refilled by TBHP.

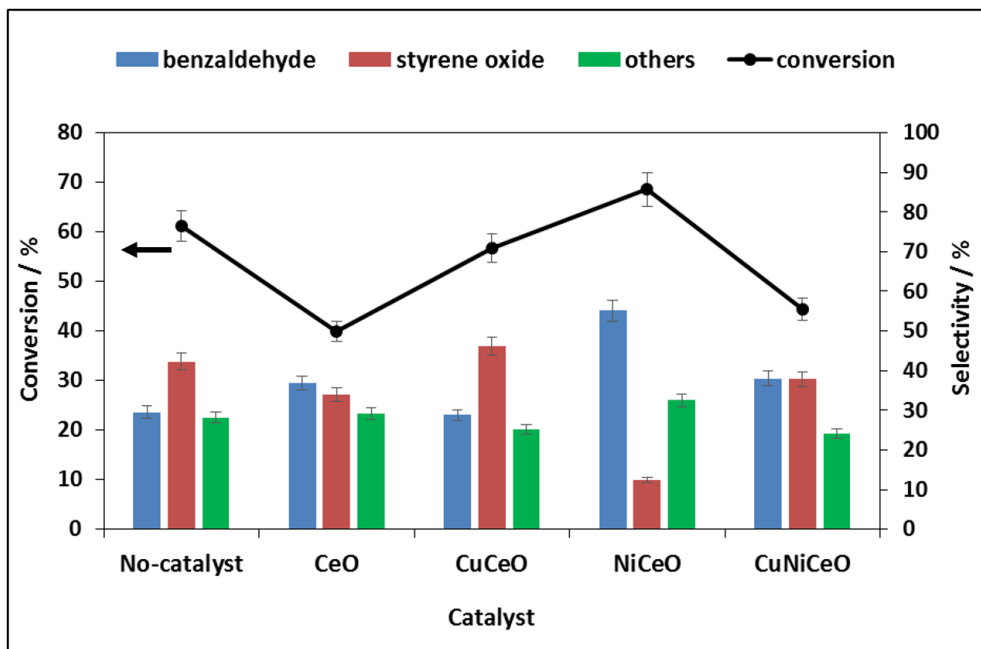


Fig. 4. Styrene conversion and product selectivity obtained for the different catalysts after 24 hours at 60 °C. Reaction conditions: 0.5 mmol styrene, 3 equiv. TBHP, 50 mg catalyst, 5 mL CH₃CN. Others: benzoic acid, 1-phenylethane-1,2-diol, acetophenone, phenyl acetaldehyde.

4 Summary and conclusion

Heterogeneous mixed metal ceria catalysts have been successfully synthesized and characterized and were found to be active in the oxidation of styrene. Conversion was found to increase when nickel or copper were added into the ceria lattice. Although the catalyst systems yielded more other products, benzaldehyde and styrene oxide were still produced in measurable quantities. Further studies are required in order to determine the role of the metals in the lattice as well as exploration of less harsh co-oxidants.

Acknowledgements

The authors would like to thank the National Research Foundation for financial support and the Microscopy and Microanalysis Unit (University of KwaZulu-Natal) for SEM and TEM analysis.

References

1. E. Novitskaya, J. P. Kelly, S. Bhaduri and O. A. Graeve, *Int. Mat. Rev.* **66** 188-214 (2021).
2. A. S. Varma, A. S. Mukasyan, K. V. Rogachev, V. Manukyan, *Chem. Rev.* **116** 14493–14586 (2016).
3. A. Khort, K. Podbolotov, R. Serrano-García, Y. Gun'ko, *Inorg. Chem.* **57** 1464-1473 (2018).

4. O. Thoda, G. Xanthopoulou, G. Vekinis, A. Chroneos, *Adv. Eng. Mater.* **20** 18-47 (2018).
5. F. Deganello, A. K. Tyagi, *Prog. Cryst. Growth Charact. Mater.* **64** 23–61 (2018).
6. E. Carlos, R. Martins, E. M. C. Fortunato, R. Branquinho, *Chem. Eur. J.* **26** 9099-9125 (2020).
7. S. A. Jasim, P. Machek, W. K. Abdelbasset, M. Jarosova, H. S. Majdi, A. D. Khalaji, *Appl. Phys. A* **128** 475 (2022).
8. M. N. Z. Ahmed, K. B. Chandrasekhar, A. A. Jahagirdar, H. Nagabhushana, B. M. Nagabhushana, *J. Mater. Environ. Sci.* **9** 2567-2574 (2018).
9. S. Khort, S. Roslyakov, P. Loginov, *Nano-Struct. Nano-Objects* **26** 100727 (2021).
10. A. Sdobnyakov, V. Khort, K. Myasnichenko, E. Podbolotov, A. Romanovskaia, D. Kolosov, D. Sokolov, V. Romanovski, *Comput. Mater. Sci.* **184** 109936 (2020).
11. S. T. Aruna, A. S. Mukasyan, *Curr. Opin. Solid State Mater. Sci.* **12** 44-50 (2008).
12. K. C. Patil, S. T. Aruna, T. Mimani, *Curr. Opin. Solid State Mater. Sci.* **6** 507-512 (2002).
13. K. C. Patil, S. T. Aruna, S. Ekambaram, *Curr. Opin. Solid State Mater. Sci.* **2** 158-165 (1997).
14. C. C. Hwang, T. Y. Wu, J. Wan, J. S. Tsai, *Mater. Sci. Eng. B* **111** 49-56 (2004).
15. C. T. Campbell, C. H. F. Peden, *Science* **309** 713-714 (2005).
16. M. A. Andrade, L. M. D. R. S. Martins, *Molecules* **26** 1680 (2021).
17. J. Liu, Z. Wang, P. Jian, R. Jian, *J. Colloid Interface Sci.* **517** 144-154 (2018).
18. Z. Li, M. Di, Y. Zhang, B. Zhang, Z. Zhang, Z. Zhang, A. Li, S. Qiao, *ACS Appl. Polym. Mater.* **4**, 1047-1054 (2022).
19. J. Valand, H. Parekh, H. B. Friedrich, *Catal. Commun.* **40** 149-153 (2013).
20. C. Liu, Y. Du, W. Zhuang, H. Xia, Q. Xie, *Acta Oceanol. Sin.* **32** 1-7 (2013).
21. J. Liu, H. Wang, P. Jian, *Catal. Lett.* **69** 280 (2022).
22. L. Nie, K. K. Xin, W. S. Li, X. P. Zhou, *Catal. Commun.* **8** 488-492 (2007).
23. L. Ju, Z. Li, S. Xu, Q. Li, *Carbon Nanostruct.* **25** 335-341 (2017).
24. A. Patel, S. Pathan, *Ind. Eng. Chem. Res.* **51**, 732-740 (2012).
25. N. Tien Thao, L. T. Kim Huyen, *Chem. Eng. J.* **279** 840-850 (2015).
26. S. J. Saadoon, M. Jarosova, P. Machek, M. M. Kadhim, M. H. Ali, A. D. Khalaji, *J. Chin. Chem. Soc.* **69**, 280-288 (2022).
27. T. Cwele, N. Mahadevaiah, S. Singh, H. B. Friedrich, *Appl. Catal. B: Environ.* **182** 1-14 (2016).
28. B. Li, X. Luo, Y. Zhu, X. Wang, *Appl. Surf. Sci.* **359** 609-620 (2015).
29. D. Ge, J. Wang, H. Geng, S. Lu, D. Wang, X. Li, X. Zhao, X. Cao, H. Gu, *ChemPlusChem*, **80** 511-515 (2015).
30. P. C. Selvaraj, V. Mahadevan, *J. Mol. Catal. A: Chem.* **120** 47-54 (1997).
31. S. Sharma, S. Sinha, S. Chand, *Ind. Eng. Chem. Res.* **51** 8806-8814 (2012).
32. F. Zadehahmadi, S. Tangestaninejad, M. Moghadam, V. Mirkhani, I. Mohammadpoor Baltork, A. R. Khosropour, R. Kardanpour, *J. Solid State Chem.* **218** 56-63 (2014).
33. X. Zhu, R. Shen, L. Zhang, *Chin. J. Catal.* **35** 1716-1726 (2014).
34. L. Paul, B. Banerjee, A. Bhaumik, M. Ali, *J. Solid State Chem.* **237** 105-112 (2016).

35. X. Liu, J. Ding, X. Lin, R. Gao, Z. Li, W. L. Dai, *Appl. Catal. A: Gen.* **503**, 117-123 (2015).